EXAMINATION AND ANALYSES OF A WOODEN FACE AT THE MUSEUM STORAGE AT THE FACULTY OF ARCHAEOLOGY, CAIRO UNIVERSITY

Yassin Zidan, Nesrin N.M. El Hadidi, Mourad F. Mohamed

Conservation Department, Faculty of Archaeology, Cairo University, Egypt

ABSTRACT

The aim of this paper is to examine and analyze a wooden face that was covered with a transparent layer of wax after finishing the mask. The use of wax and encaustic painting was used in Ancient Egypt during the Greco – Roman period, but it was an extremely rare technique in the Egyptian dynasties.

The wooden face that was chosen for this study was carefully examined using light microscopy to identify the wood, which proved to be native sycomore fig (*Ficus sycomorus*). Digital microscope and Scanning Electron Microscope (SEM) were used to assess decay of the outer exposed surface that had been covered in the past with a preparation layer composed of calcium carbonate. SEM micrographs showed clear decay of the cell walls due to the penetration of both the preparation layer and fungal hyphae.

Microbiological investigation indicated the presence a bacterial and fungal infestation. The wood was infected infected by *Aspergillus niger* and *Ulocladium sp* fungi and *Pediococcus dextrinicus* bacteria.

Further assessment was done by X- Ray Diffraction (XRD) to calculate the decrease of cellulose crystallinity according to Segal and Fourier Transform spectroscopy (FTIR) to detect the changes of the main wood components (cellulose, hemicellulose, lignin).

KEYWORDS: Wood Decay, XRD, FTIR, SEM, Microbiology, Cellulose Crystallinity

1. INTRODUCTION

Wooden faces were part of wooden coffins; which were designed to resemble the face of the deceased. They were attached to the coffin by wooden joints, e.g. pegs, and were covered with preparation layers usually composed of calcite (calcium carbonate), followed by a painting layer. This technique was widespread during the pharaonic ages in Egypt. The wooden face chosen for this study is stored in the museum store at the Faculty of Archaeology - Cairo University. Origin of the mask is unknown, but according to technical characteristics, it presumably dates back to the 25th or 26th pharaonic dynasty. The mask has a transparent and thin layer of beeswax, which is rare in the case of objects dating back to that period. The use of beeswax was unknown before this period, and although the technique is similar to the Fayoum Portraits technique in the Greco – Roman period, yet in Fayoum Portraits technique, the wooden faces were flat and covered with painted wax to resemble the face of the deceased. However in this wooden face the applied technique is a combination of ancient Egyptian art and Fayoum portraits.

Examination and analysis of the wooden face had been conducted to find out the components of deterioration. Light microscope was used to identify the type of wood by preparing longitudinal and cross section glass slides which were compared with previously published data (Crivellaro and Schweingruber 2013) (Timar, et al. 2010). Scanning Electron Microscope (SEM) was used to examine the micro deterioration in the anatomical structure of the wood and the decay of microorganisms (Blanchette 2000) (Hamed, Ali and El Hadidi 2012). Fourier Transform Infrared Microscopy (FTIR) was used to study the changes in wood chemistry compounds (cellulose- hemicellulose- lignin) following decay. These compounds have characteristic absorption spectra in FTIR analysis (Muller G, et al. 2009). Generally, O-H stretching absorption bands (around 3400 cm^{-1}) and C-H absorption bands (around 2927 cm^{-1}) have contributions from all the chemical components (Jiangtao, Dong and Li 2012) (Bodirlau 2007). C-H absorption bands were divided into four bands, the first is $C-H_3$ asymmetric stretching band at (2950-2970), second $C-H_2$ asymmetric stretching band at (2915-2935), third $C-H_3$ symmetric stretching band at (2860-2880), the last one is $C-H_2$ symmetric stretching band at (2845-2865) (Esteves B. 2013). Important peaks were assigned as follows: (1730-1740) (unconjugated C=O in hemicelluloses) (Ray, et al. 2012) (Temiz, et al. 2007), and the band at (1640) for absorbed H-O–H (Picollo, et al. 2011). Absorption bands at (1610-1500) are characteristic to lignin,

whereas the bands at (1590-1610) refer to aromatic C=C stretching (Syringyl > Guaiacyl) and the bands at (1505-1515) refer to aromatic C=C stretching (Syringyl < Guaiacyl). (Huang, et al. 2013) (Rana, et al. 2010), while the absorption bands at (1460-1470) refer to C-H bending bands in cellulose and hemicellulose (Pucetaite 2012) and C-H bending bands in cellulose and aromatic skeletal in lignin are at (1425) (Atalla 2010). The absorption bands at (1346-1384) refer to C-H and O-H bending bands in cellulose and hemicellulose (Pucetaite 2012), at (1315-1335) the bands of $C-H_2$ in amorphous cellulose and O-H bending bands in cellulose and hemicellulose (Parida, Dash and Pradhan 2015) and C-O stretching band for lignin (Syringyl only) (Tolvaj 2009). There is a C-O stretching band for lignin (Guaiacyl only) and hemicellulose at (1245-1270) (Agresti, et al. 2013). The absorption bands at (1221-1235) are C-O stretching band for lignin (Syringyl) and O-H bending band for hemicellulose and cellulose (Naumann, et al. 2007) and C- O stretching for hemicellulose at (1244) (Rana, et al. 2010). The bands at (1205) refer to O-H bending band for hemicellulose and cellulose, C- O stretching for cellulose and C-H bending in plane for lignin (Guaiacyl) at (1140) (Esteves B. 2013), C-O-C stretching for characteristic spectra of cellulose polymerization at (1150-1165) (Poletto, Zattera and and Santana 2012), C-H bending in plane for lignin (Syringyl) and C-O stretching for secondary alcohol at (1125-1130) (Huang, et al. 2013), C- O stretching for hemicellulose and cellulose at (1060-1117) (Genestar and Palou 2006) and (1084) (Pandey and Pitman 2003), aromatic C-H Bending out of plane for lignin at (800-875) and C-H rocking for cellulose at (800-950) (Huang, et al. 2013).

Analyses with X-Ray Diffraction were used to identify the compounds of the white layer on the wooden face and to measure the crystallinity of cellulose, which is an important indicator of wood decay. The crystalline structure of cellulose has been studied for a long time, and dates back to the 19th century (Carl von Nageli.1858) (Ciolcu, Ciolaui and Opa 2001). It is well known that crystallinity of cellulose can be measured using quite a number of methods such as X-ray diffraction, solid state ^{13}C CP-MAS NMR (Park, et al. 2009), Fourier transform infrared (FT-IR) spectroscopy (Akerholm, Hinterstoisser and Salmen 2004) and Raman spectroscopy (Schenzel 2005), (Terinte, Ibbett and Schuster 2011) (Zugenmaier 2008). However, the X-Ray Diffraction method is the widespread one. There are many methods to determine the crystallinity of cellulose by X-Ray diffraction and research is still ongoing to find the best ways to determine the crystallinity of cellulose by X-Ray diffraction method. The most common methods that were carried out by various scientists

(Terinte, Ibbett and Schuster 2011) (Bansal, et al. 2010) are as follows:

1. Hermans-Weidinger method (Hermans and Weidinger 1948)

2. Segal method (Peak height) (Segal, et al. 1958)

3. Wakelin method (1959) (Bansal, et al. 2010)

4. Ruland (1961) (Ruland 1961) –Vonk (1972) (Vonk 1972) method.

5. Jayme-Knolle method (Jayme and Knolle 1964)

6. Chung and Scott method (Chung and Scott 1973)

7. Soltys method (Soltys, Lisowski and Knapczyk 1984)

8. Polizzi method (Polizzi, et al. 1990)

9. Ibbett method (curve fitting) (Ibbett, Domvoglou and Phillips 2008).

All of these methods depended on crystalline peaks at (14.5±0.2°), (16.5±0.2°), and (22-24°) and amorphus area at (18±0.2°) (Howell, Hastrup and Jellison 2007).

Segal method is the most widespread and was applied in this study.

2. MATERIALS AND METHODS

2.1. The Archaeological Wooden Face

The wooden face in this study is stored in the museum store at the Faculty of Archaeology- Cairo University. It was made from wood, covered with a white gesso layer and a thin transparent wax layer (Fig. 1, 2).

Figure 1. Front of the wooden face

Figure 2. Back of the wooden face

2.2. Light Microscope

Wooden slides were prepared according to Barbotin 2014. The photos of wood sections were taken by Leica - ICC 50 – HD Light Microscope at the Faculty of Agriculture at Cairo University. Egypt.

2.3. Scanning Electron Microscope (SEM)

Scanning electron Microscopic analysis of the samples was carried out using (JEOL JSM S400LV EDX Lin l ISIS-Oxford high vacuum) at the Faculty of Science, Assiut University. Egypt. The samples were coated with gold.

2.4. Fourier Transform Infrared Microscopy (FTIR)

FTIR spectra of wood samples were measured on a Nicolet 380 FT-IR Spectrometer, in the frequency range of 4000 - 400 cm^{-1}, in transmission mode using the KBr pellet technique at the National Institute for Standards (NRC) in Cairo, Egypt. Peak heights and width of absorption bands were measured by Essential FTIR software (version 310.041).

2.5. X-Ray Diffraction (XRD)

Chemical composition of the compounds percentages of the preparation layers and measurements of the crystallinity of cellulose in the wood samples were obtained by X-Ray powder diffraction using a Philips Analytical X-Ray B.V. (type PW 1840 diffractometer, Netherland) with a Cu tube anode, Generator tension (kv) is (40) - Generator current (mA) is (25). Wavelength alpha1 is (1.54056), wavelength alpha2 is (2.54439). Receiving slit is (0.2),

intensiy ratio (alpha2/ alpha1) is (0.500). Full scale of recorder is ({kcounts/s}:10). Start angle {2θ} is (10.00), end angle {2θ} is (30.00).

Step size is ({2θ} : 0.010). Type of scan is continuous. Time per step ({s} : 0.100). Peak positions defined by top smoothed peak. Threshold is (0). Minimum peak tip width is (0.00), peak base width is (2.00), minimum peak tip width is (1.00) and minimum significance is (0.95). Peaks were identified and measured by using Match 3 + PDF4 2015 software program.

2.6. Isolation and identification of fungi

Fungal studies of wood samples to isolate purified and identified fungi were conducted at the Microbiology Laboratory of the Faculty of Archaeology in Cairo University, Egypt. Swab sampling technique was used, and the samples were cultivated on potato dextrose agar (PDA) medium containing (200 g) of potato starch, (20 g) of dextrose, (15 g) of agar and (1000 ml) of distilled water in the Petri dishes (Atlas 2010) (Mueller, Bills and Foster 2004). After 14 days of incubation at (25-30 ℃), identification was carried out according to various references (Kird, et al. 2008) (Samson, et al. 2010) and (Williams and Buchanan 2001).

2.7. Isolation and identification of bacteria

Bacterial studies of wood samples were isolated and purified at the Microbiology Laboratory of the Faculty of Agriculture at Cairo University, Egypt. The samples were cultivated on tryptone soya agar (TSA) medium (Abrusci, et al. 2005) (Atlas 2010). After 14 days of incubation at 30℃, identification was carried out at Microbiology Laboratory of the Faculty of Science at Cairo University, Egypt.
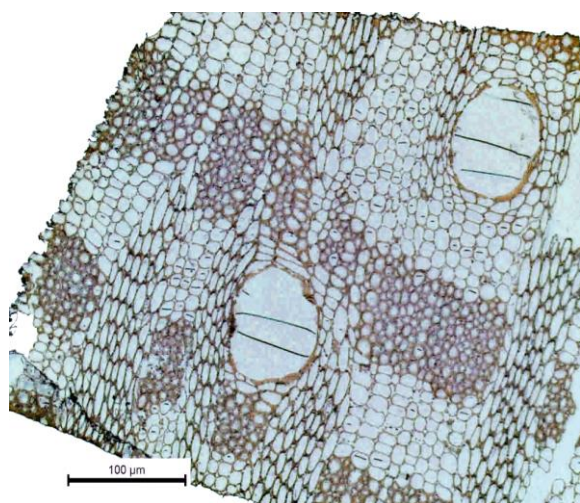

Figure 3. Light microscope image of transverse section of sycamore wood (Ficus sycomorus) taken from the wooden face, bar 100 μm

3. RESULTS AND DISCUSSION

3.1. Light Microscope

Identification of wood sample type according to the light microscope images of wood slides shows that, the wooden face was made from a local Egyptian hardwood type of (*Ficus sycomorus*). Tangential section (Fig. 3) and longitudinal section (Fig. 4) show the characteristic structure of wide-banded fibres and axial parenchyma, large vessels and multiseriate rays.
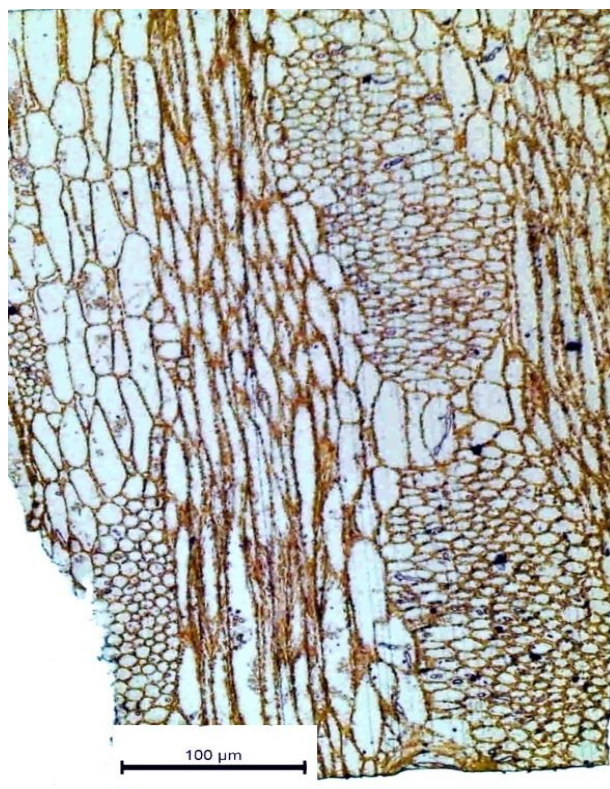

Figure 4. Light microscope images of tangential section of sycomore wood (Ficus sycomorus) taken from the face, bar 100 μm

3.2. Scanning Electron Microscope (SEM)

SEM micrographs of wood samples taken from the wooden face show the degrading effect of $CaCO_3$ preparation layer (El Hadidi and Hamed, in press). The preparation layer is finely distributed on the outer wood surface, and is trapped between cells (fig. 5 A). Separation between wood cells is due to lose of middle lamella region, that leads to loss of coherence in wood structure causing either fracture or delamination (fig. 5 B) and eroded parts of the cell wall. In addition to separations, cracks and fissures occurring within the cell wall layers (fig. 5 C).
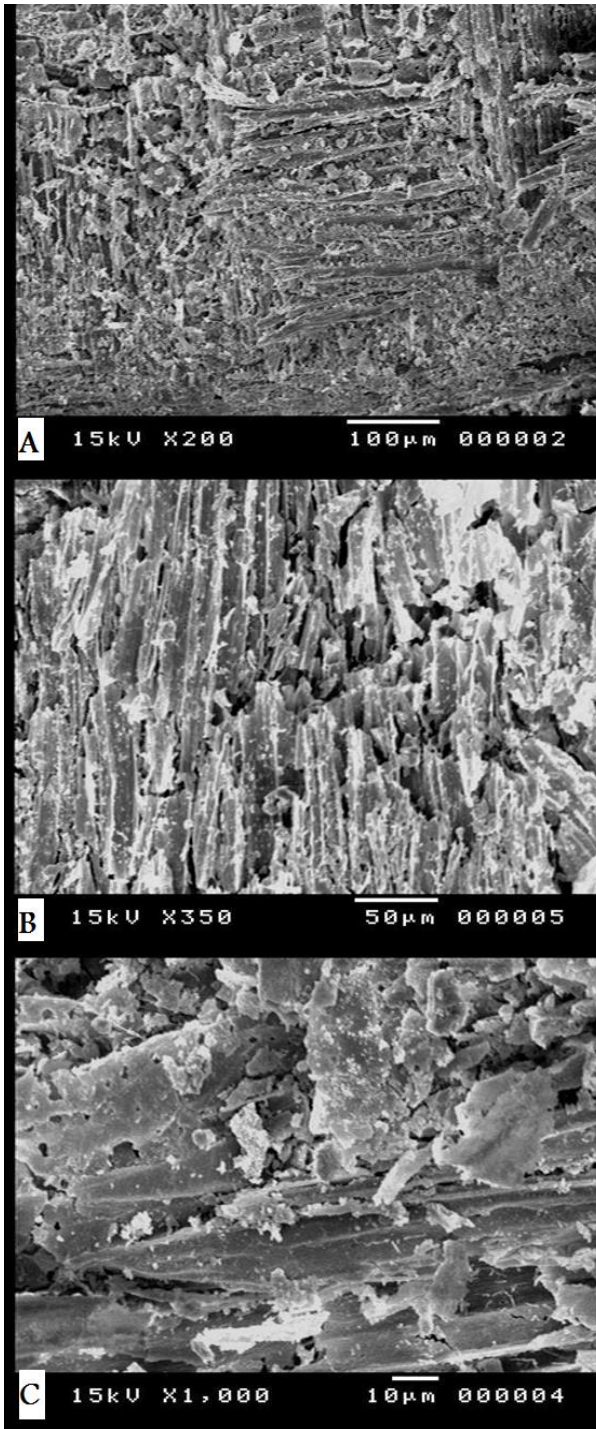
Figure 5. SEM micrographs: (A) The preparation layer slightly covering the wood tracheids, (B) Separation between wood cells. (C) Fractured and eroded parts of the cell walls that were covered with CaCO₃.
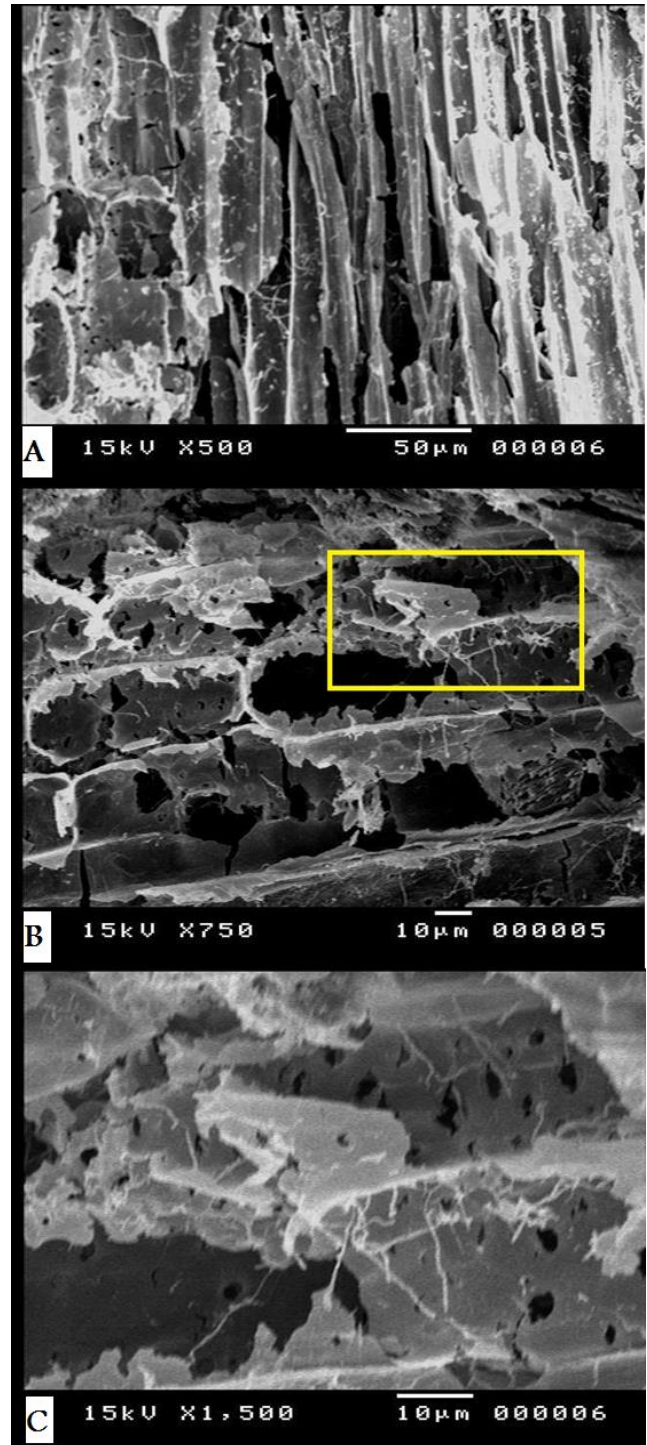

Figure 6. SEM micrographs: (A) Breakdown of the wood cells, (B) Advanced stage of decay resulted in the gradual breakdown of the wood cell wall layers. (C) Detail from previous image.

Breakdown of the wood cells, which have become easily fragmented, as well as the cell wall layer erosion due to the extensive biodegradation where hyphae are evident (fig. 6 A). Advanced stage of decay resulted in the gradual breakdown of the wood cell wall layers (fig. 6 B) and can be clearly seen at higher magnification of the hyphae penetrating the pits between cells causing erosion of the cell walls (fig. 6 C)

3.3. Fourier Transform Infrared Microscopy (FTIR)

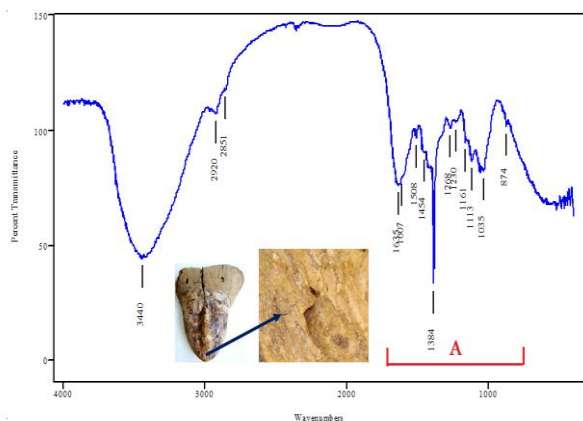FTIR analyses results of wood sample from the object are shown in (Fig. 7, 8) (table 1).

Figure 7. FTIR Transmittance Spectra of wooden Face Sample from 400 to 4000 cm⁻¹, where A represents the major wood components in the fingerprint region from 800 to 1800 cm⁻¹.
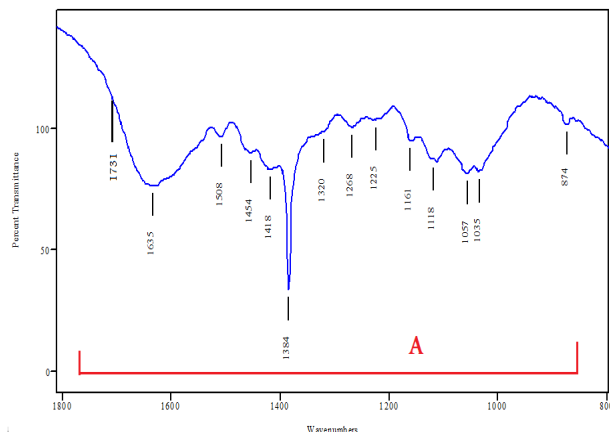

Figure 8. FTIR Transmittance Spectra of wooden Face Sample from 800 to 1800 cm⁻¹ (fingerprint area).

Table 1: The FTIR analysis results of wood sample.

| Wave-number (cm⁻¹)	Functional group bands	Assignment
3440	OH stretching	Cellulose, Lignin and hemicellulose
2920	C-H_2 asymmetric stretching	Cellulose, Lignin and hemicellulose
2851	C-H_2 symmetric stretching	Cellulose, Lignin and hemicellulose
1731	Unconjugated C=O stretching as a shoulder	Xylan and hemicellulose
1635	Conjugated C=O stretching + H-O-H absorption	Due to oxidation of cellulose
1607	C=C stretching of the aromatic ring	Lignin (Syringyl > Guaiacyl)
1508	C=C stretching of the aromatic ring	Lignin (Syringyl < Guaiacyl)
1454	CH_3 bending	Cellulose, Lignin and hemicellulose
1418	CH_2 bending	Cellulose (crystallized and amorphous)
1384	CO_3 stretching + CH_2 bending	Calcite (Gesso) + Cellulose
1330	OH bending + C-O stretching	Cellulose (amorphous) + Lignin (Syringyl)
1268	C-O stretching	Lignin (Guaiacyl)
1225	C-O stretching	Lignin (Syringyl)
1161	C-O-C bridge oxygen stretching	Cellulose
1118	C-O stretching	Cellulose and hemicellulose
1056	C-O stretching	Cellulose, lignin and hemicellulose
1035	C-O stretching	Cellulose and hemicellulose
874	C-H aromatic bending out of plan + C-H rocking	Lignin + cellulose
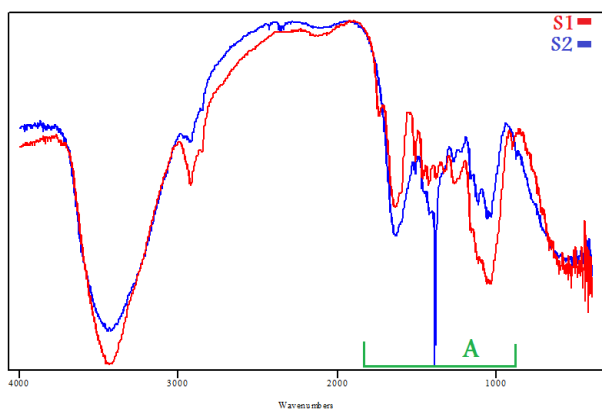
Figure 9. FTIR Spectra Transmittance of wooden Face Sample (S2) and the control sample (S1) from 400 to 4000 cm⁻¹.
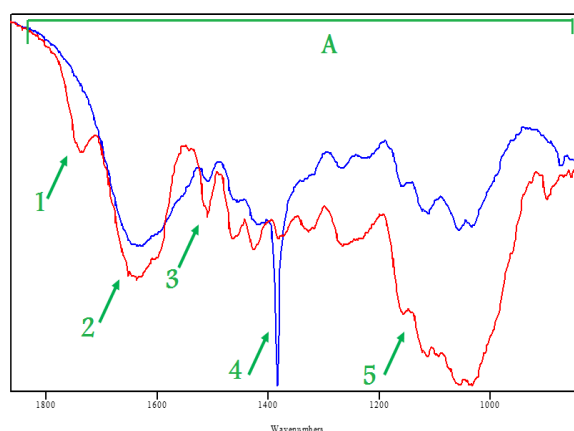

Figure 10. FTIR Spectra Transmittance of wooden Face Sample and the control sample from 800 to 1800 cm⁻¹ (fingerprint area).

FTIR analysis of the decayed sample and a new one from the same type of wood (*Ficus sycomorus*) as a control sample (fig. 9, 10) were compared to understand the changes of chemical compounds of wood exposed to different decay factors.

The results of FTIR analysis of wood in (fig. 9, 10) showed that most changes occurred in the chemical compounds in the area around (1000-1800 cm^{-1}) (fig (10). There are five major differences between the archaeological sample and control sample:

1) Decrease of the intensity band of unconjugated C=O stretching around (1730 cm^{-1}) in the decayed sample which appears as a shoulder, explained by the decrease in hemicellulose amount in archaeological sample.

2) Decrease of the intensity band of water absorption around (1640 cm^{-1}) and decrease in O-H stretching band around (3300-3400 cm^{-1}) (fig. 9) because of the loss of water due to the dry storage conditions.

3) Decrease of C=C stretching band around (1508 cm^{-1}) due to loss of lignin according to fungal degradation (Darwish, El Hadidi and Mansour 2013).

4) Increase of the band at (1384 cm^{-1}) due to the remains of calcite from gesso layer covering the wooden face.

5) Decrease of C-O-C stretching bands around (1160 cm^{-1}), indicate advanced breaking of cellulose chains and the occurrence of depolymerisation (Darwish, El Hadidi and Mansour 2013).

3.4. X-Ray Diffraction (XRD)

According to the results of X-ray Diffraction analysis, the white layer (gesso) that covered the wood surface was composed of Calcite (Calcium Carbonate CaCO$_3$) (Fig. 11).
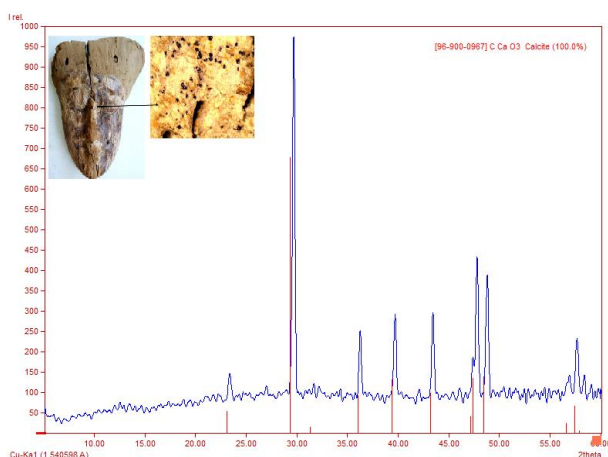

Figure 11. X-ray diffraction pattern of the white layer (gesso) covered the wooden face.

X-ray diffraction was also used to measure crystallinity index of cellulose according to Segal equation.

$$Cr = 100 \times \frac{I_{002} - I_{am}}{I_{002}}$$

Where: (Cr) expresses the crystallinity of cellulose (I$_{002}$) express the maximum intensity of the crystallinity peak at (2θ = 22-24°) and (I$_{am}$) represents the intensity of diffraction of the non-crystalline cellulose at (2θ = 18°) (fig. 12).
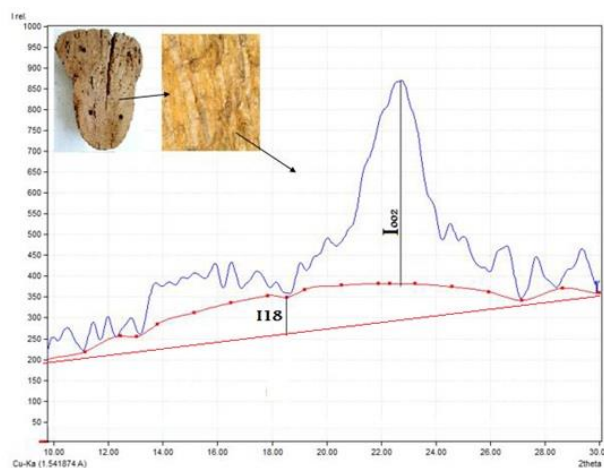

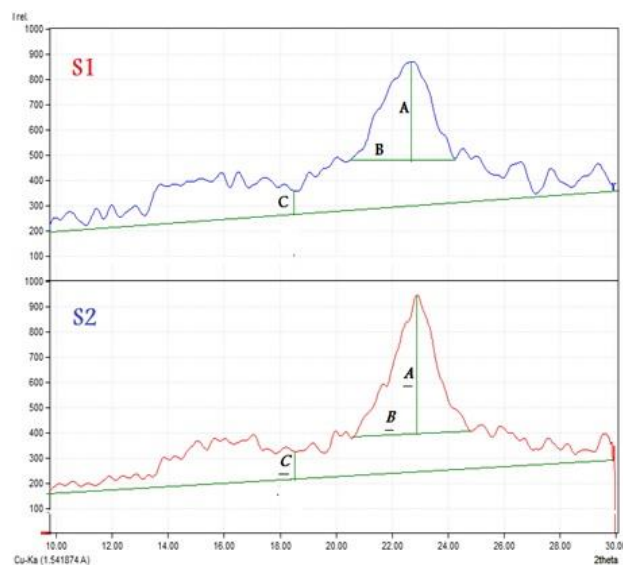*Figure 12. X-ray diffraction of the wood from the wooden face to measure the crystallinity of cellulose.*

Figure 13. X-ray diffraction pattern of wood from the wooden face (S1) and Ficus sycomorus control sample (S2) explaining how the crystallinity peaks of cellulose are measured.

Comparison between the cellulose crystallinity of the wooden face sample (S1) and the control sample of the same wood type (*Ficus sycomorus*) (S2) indicated a decrease in the crystalline index of the decayed sample (fig. 13) (table 2), where (A) expresses the maximum intensity of the crystallinity peak at (2θ = 22.6°), (B) refers to peak width, (C) represents the in-

tensity of diffraction of the non-crystalline cellulose at (2θ = 18°) and (Cr) expresses the crystallinity of cellulose. The decrease of the decayed crystallinity is due to the decay by bacteria, fungi and weathering.

Table 2: The results of comparing crystallinity

Symbol	S_1	S_2
A	380	522
B	3.5°	4.2°
C	112	126
Cr	70.5%	77.2%

3.5. Identification of Fungi

The results of fungal identification after isolation (fig. 14), show that the wooden face was infected by *Aspergillus niger* (fig. 15) and *Ulocladium sp* fungi (fig. 16).
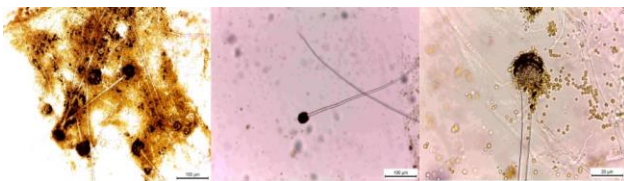

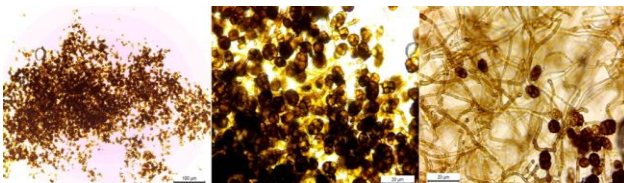*Figure 14. Isolation of fungi*

Figure 15. Aspergillus niger

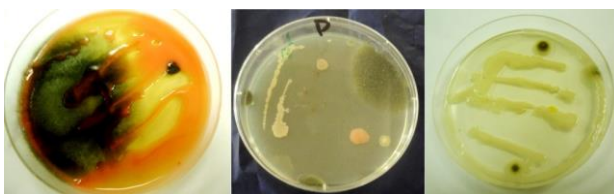
Figure 16. Ulocladium sp

Figure 17. Isolation of bacteria

3.6. Identification of Bacteria

The results of bacterial identification after isolation (fig. 17), show that the wooden face was infected

by *Pediococcus dextrinicus* (Coster and White 1964) (Haakensen, et al. 2009). Morphology characters and physiology of *Pediococcus dextrinicus* are shown in table 3.

Table 3: The results of identification of bacteria.

Bacteria Type	*Pediococcus dextrinicus* (Coster and White 1964)
Morphology	Cocci
Gram reaction	G+
Characters and physiology	- Type strain ATCC 33087. - Smooth round colonies. - Spherical cells, division occurs alternately in two planes at right angles to form tetrads. - Single cells are rare and chains of cells are not formed. - Motility: nonmotile. - Spores not formed. - Facultative anaerobes. - Chemoorganotrophs requiring a rich medium; having complex growth factors and amino acid requirements. - Optimum temperature range: 30-35°C. - Growth at 40°C: (+). - Catalase: (-). - Optimum pH 6.5. - Growth at pH 8.5 (-). - Acid production from: • Maltose, dextrin and starch: (+) Arabinose and trehalose: (-).

4. CONCLUSION

The chemical composition of wood is easily affected by endless decay factors that continuously attack wood. It is incorrect to believe that wood stored away unexposed to severe decay factors will not degrade. Every type of wood continues to decay in different ratios depending on many environmental factors. In this paper a correlation between common decay factors and decay assessment is undergone. This type of assessment needs to be applied in future research with the aim of understanding the decay pattern of wood components.

REFERENCES

Abrusci, C., Martı, A., Del Amob, A., Catalina, F., Collado, J., & Platas, G. (2005). Isolation and identification of bacteria and fungi from cinematographic films. *International Biodeterioration & Biodegradation 56*, 58–68.

Agresti, G., Bonifazi, G., Calienn, L., Capobianco, G., Monaco, A., Pelosi, C., and Serranti, S. (2013). Surface Investigation of Photo-Degraded Wood by Colour Monitoring, Infrared Spectroscopy, and Hyperspectral Imaging. *Journal of Spectroscopy*, 1-13.

Akerholm, M., Hinterstoisser, B., & Salmen, L. (2004). Characterization of the crystalline structure of cellulose using static and dynamic FT-IR spectroscopy. *Carbohydrate Research 339*, 569–578.

Atalla, U. P. (2010). Vibrational Spectroscopy. In C. Heitner, D. Dimmel, & J. Schmidt, *Lignin and lignans : advances in chemistry* (pp. 104-134). USA: Taylor and Francis Group, LLC.

Atlas, R. (2010). *Handbook of Microbiological Media.* Washington, D.C.: Fourth Edition, CRC Press.

Bansal, P., Hall, M., Realff, M., Lee, J., & Bommarius, A. (2010). Multivariate statistical analysis of X-ray data from cellulose: A new method to determine degree of crystallinity and predict hydrolysis rates. *Bioresource Technology 101*, 4461–4471.

Barbotin, S. (2014). *Micro-preparation of wooden samples to study the distribution of natural glue systems in wood.* BFH AHB Institut.

Blanchette, R. (2000). A review of microbial deterioration found in archaeological wood from different environments. *International Biodeterioration & Biodegradation 46*, 189-204.

Bodirlau, C. T. (2007). Fourier Tranceform Infrared Spectroscopy and Thermal Analysis of Lignocellulose Fillers Treated with Organic Anhydrites. *the 8th International Balkan Workshop on Applied Physics.* Constanţa, Romania: Rom. Journ. Phys.

Chung, F., & Scott, R. (1973). A new approach to the determination of crystallinity of polymers by X-ray diffraction. *Journal of Applied Crystallography 6*, 225–230.

Ciolcu, D., Ciolaui, F., & and opa, V. (2001). Amorphous Cellulose Structure and Characterization. *Cellulose Chem. Technol., 45 (1-2)*, 13-21.

Crivellaro, A., & Schweingruber, F. (2013). *Atlas of Wood, Bark and Pith Anatomy of Eastern Mediterranean Trees and Shrubs.* Berlin: Springer.

Darwish, S., El Hadidi, N., & Mansour, M. (2013). The Effect of Fungal Decay on Ficus sycomorus wood. *International Journal for Conservation Science*, 271-282.

El Hadidi, N. M. N., Hamed, S. A. M. (in press). The effect of Preparation layers on the Anatomical Structure and Chemical Composition of Native Egyptian Wood, In: *Proceedings First Vatican Coffin Conference*, Vatican Museums Conference Hall, 19 - 22 June 2013

Esteves B., A. M. (2013). Chemical Changes of Heat Treated Pin and Eucalypt Wood Monitored by FTIR. *Maderas. Ciencia y tecnología 15(2)*, 245-258.

Genestar, C., & Palou, J. (2006). SEM–FTIR spectroscopic evaluation of deterioration in an historic coffered ceiling. *Anal Bioanal Chem 384*, 987–993.

Haakensen, M., Dobson, M., Hill, J., & Ziola, P. (2009). Reclassification of Pediococcus dextrinicus (Coster and White 1964) Back 1978 (Approved Lists 1980) as Lactobacillus dextrinicus combnov., and emended description of the genus. *International Journal of Systematic and Evolutionary Microbiology. 59*, 615–621.

Hamed, S., Ali, M., & El. Hadidi, N. (2012). Using SEM in monitoring changes in archaeological wood: A review. *Current Microscopy Contributions to Advances in Science and Technology*, 1077-1084.

Hermans, P., & Weidinger, A. (1948). X-Ray Studies on the Crystallinity of Cellulose. *Journal of Polymer Science Volume 1*, 135-144.

Howell, C., Hastrup, A., & Jellison, J. (2007). The use of X-ray diffraction for analyzing biomodification of crystalline cellulose by wood decay fungi. *the 38th Annual Meeting Jackson Lake Lodge*, (pp. 1-16). Wyoming, USA.

Huang, Y., Wang , L., Chao, W., Sarip, D., Nawawi, Akiyama, Y., Matsumoto, Y. (2013). Analysis of Lignin Aromatic Structure in Wood Based on the IR Spectrum. *Journal of Wood Chemistry and Technology.*, 294-303.

Ibbett, R., Domvoglou, D., & Phillips, D. (2008). The Hydrolysis and Recrystallisation of Lyocell and Comparative Cellulosic Fibres in Solutions of Mineral Acid. *Cellulose 15*, 241-254.

Jayme, G., & Knolle, H. (1964). Introduction into Empirical X-ray Determination of Crystallinity of Cellulose Materials. *Das Papier 18*, 249-255.

Jiangtao, S., Dong, X., & Li, J. (2012). FTIR Studies of the Changes in Wood Chemistry from Wood Forming Tissue under Inclined Treatment. *International Conference on Future Energy Environment, and Materials* (pp. 758 – 762). Elsevier.

Kird, P., Cannon, P., David, J., & Stalpers, J. (2008). *Dictionary of the fungi.* Wallingford: 10th Edition, CABI publishing.

Mueller, G., Bills, G., & Foster, M. (2004). *Biodiversity of fungi, inventory and monitoring methods.* U.S.A: Elsevier Academic Press.

Muller G, Schopper C, Vos H, Kharazipour A, & Polle A. (2009). FTIR-ATR Spectroscopic Analysis of Changes in Wood Properties During Particle and Fiberboard Production of Hard and Soft Wood Trees. *Bioresources*, 49-71.

Naumann, A., Peddireddi, S., Kües, U., & and Polle, A. (2007). Fourier Transform Infrared Microscopy in Wood Analysis. In U. Kües, *Wood Production, Wood Technology, and Biotechnological Impacts* (pp. 179-196). Göttingen: Universitätsverlag Göttingen.

Pandey, K., & Pitman, A. (2003). FTIR studies of the changes in wood chemistry following decay by brown-rot and white-rot fungi. *International Biodeterioration & Biodegradation 52*, 151 – 160.

Parida, C., Dash, K. S., & Pradhan, C. (2015). FTIR and Raman Studies of Cellulose Fibers of Luffa cylindrica. *Open Journal of Composite Materials 5*, 5-10.

Park, S., Johnson, D., Claudia, I., Parilla, P., & Davis, M. (2009). Measuring the crystallinity index of cellulose by solid state 13C nuclear magnetic resonance. *Cellulose 16*, 641–647.

Picollo, M., Cavallo, E., Macchioni, N., Pignatelli, O., Pizzo, B., & Santo, I. (2011). Special Characterization of Ancient Wooden Artefacts with the use of Traditional IR Techniques and Art Device : A Methodologyical Approach. *e-Pereservation Science*, 23-28.

Poletto, M., Zattera, A. G., & and Santana, R. (2012). Structural Differences Between Wood Species Evidence from Chemical Composition FTIR Spectroscopy, and Thermogravimetric Analysis. *Journal of Applied Polymer Science, Vol. 126*, 336–343.

Polizzi, S., Fagherazzi, G., Benedetti, A., & Battagliarin, M. (1990). A fitting method for the determination of crystallinity by means of X-ray diffraction. *Journal of Applied Crystallography 23*, 359–365.

Pucetaite, M. (2012). *Archaeological wood from the Swedish warship Vasa studied by infrared microscopy.* Department of Physics, Lund University.

Rana, R., Langenfeld, R., Finkeldey, R., & Polle, A. (2010). FTIR spectroscopy, chemical and histochemical characterisation of wood and lignin of five tropical timber wood species of the family of Dipterocarpaceae. *Wood Sci Technol*, 225–242.

Ray, R., Majumder, N., Chowdhury, C., & Jana, T. (2012). Wood chemistry and density: An analog for response to the change of carbon sequestration in mangroves. *Carbohydrate Polymers 90*, 102– 108.

Ruland, W. (1961). X-ray Determination of Crystallinity and Diffuse Disorder Scattering. *Acta Crystallogr. 14*, 1180-1185.

Samson, R., Houbraken, J., Frisvad, J., & Andersen, B. (2010). *Food and indoor fungi.* Utrecht, The Netherlands: Laboratory Manual Series, CBS-KNAW Fungi Biodiversity centre Utrecht, The Netherlands, An institute of the Royal Netherlands Academy of Arts and Sciences.

Schenzel, K. F. (2005). New Method for Determining the Degree of Cellulose I Crystallinity by means of FT Raman Spectroscopy. *Cellulose 12*, 223-231.

Segal, L., Creely, J. J., Martin, A. M., & Conrad, C. (1958). An Empirical Method for Estimating the Degree of Crystallinity of Native Cellulose Using the X-Ray Diffractometer. *Textile Research.29*, 786-794.

Soltys, J., Lisowski, Z., & Knapczyk, J. (1984). X-ray diffraction study of the crystallinity index and the structure of the microcrystalline cellulose. *Acta Pharmaceutica Technologica 30*, 174–180.

Temiz, A., Terziev, N., Eikenes, M., & Hafren, J. (2007). Effect of accelerated weathering on surface chemistry of modified wood. *Applied Surface Science 253*, 5355–5362.

Terinte, T., Ibbett, R., & Schuster, K. C. (2011). Overview Native Cellulose and Microcrystalline Cellulose I Structure Studied by X-Ray Diffraction (WAXD): Comparison Between Measurment Techniques. *Lenzinger Berichte 89*, 118-131.

Timar, M., Gurau, L., Coinca, M., & Projan, M. (2010). Wood Species for the Bedermeier Furniture a Microscopic Characterisation for Scientific Conservation. *Intrnational Journal of Conservation Science*, 3-12.

Tolvaj, L. (2009). Monitoring of Photodegradation for Wood by Infrared Spectroscopy. *International Conference on Wooden Cultural Heritage.* Hamburg, Germany.: Wood Science for Conservation of Cultural Heritage.

Vonk, C. G. (1972). Computerization of Ruland's X-ray Method for Determination of the Crystallinity in Polymers. *Appl. Cryst.*, 149-152.

Williams, J., & Buchanan, G. (2001). *Simplified fungi identification key.* The University of Georgia, College of Agricultural & Environmental Sciences, Special Bulletin 37.

Zugenmaier, P. (2008). *Crystalline Cellulose and Derivatives: Characterization and Structures.* Berlin: Springer.